

# Incremental Step Reference Governor for Load Conditioning of Hybrid Fuel Cell and Gas Turbine Power Plants

Vasilis Tsourapas, Jing Sun, Anna Stefanopoulou

**Abstract**—A hybrid Solid Oxide Fuel Cell and Gas Turbine (SOFC/GT) system exploits the complementary features of the two power plants, where the GT recuperates the energy in the SOFC exhaust stream and thereby boosting the overall system efficiency. Through model based transient analysis, however, it is shown that the intricate coupling dynamics make the transient load following very challenging. Power shutdown has been observed when the load is changed abruptly. In this work, a novel closed-loop reference governor controller is proposed to mitigate the shutdown phenomenon. The reference governor utilizes the region of attraction of a reduced order SOFC/GT model to determine the feasibility of applying an incremental step change, subject to the constraint of no system shutdown. It is shown that with a moderate computational cost, the speed of the hybrid power system response can be improved significantly compared to the fastest conventional load filter.

**Index Terms**—SOFC, hybrid, fuel cells, dynamics, modeling, feedback control.

## I. INTRODUCTION

Integrating fuel cell based power systems with energy recuperation devices (ERDs) can further improve the already high system efficiency by reducing the exhaust energy losses. Such integration often results in hybrid power systems, of which the combination of the solid oxide fuel cell (SOFC) and gas turbine (GT) studied in this paper is a representative configuration (Fig. 1). Energy recuperation is critical in achieving high system efficiency and in assuring minimal energy losses to the environment. Fuel cell systems are ideal candidates for incorporating energy recuperation devices for several reasons. In order to assure high efficiency and to avoid hydrogen starvation, fuel cell stacks do not operate at fuel utilization ratios close to 100% [1], [2]. The existence of the unused fuel in the exhaust represents a significant opportunity for energy recovery. For the high temperature SOFCs, especially for the pressurized SOFCs, the high exhaust temperature and energy content make the energy recuperation even more attractive.

The integrated fuel cell systems with energy recuperation devices have been studied extensively in the literature, motivated by the substantial benefits of ERDs. Several studies show that the steady state efficiency increases when energy

recuperation devices are incorporated in a fuel cell system [3]. Other publications on control oriented analysis of SOFC systems identify the load following limitations and implement model predictive control schemes to resolve them [4]. On coupled SOFC/GT systems, a dynamic model of an SOFC/GT system is developed in [5]. The model is validated using experimental data provided by Siemens Westinghouse and the authors note that the model, built from first principles, can reasonably predict the dynamic performance of a complex hybrid FC/GT system. The authors of [6] develop a dynamic model of an SOFC/GT system and evaluate the matching between that model and a linearized version of the same model. They note that the linear and nonlinear model responses match only for small range of variations (less than 10%) in the inputs. Thus, the nonlinearities cannot be ignored in the performance analysis. Finally, the authors of [7] pointed out that: “*With a given constant generator power, the system is at an unstable equilibrium. Departing from steady-state, for example, a step increase of the generator power will lead to deceleration of the shaft speed. No new equilibrium will be found within the valid bounds of shaft speed*”. The authors note that shaft speed regulation can be achieved via “*trial-and-error tuning of a PID controller*”, using as feedback the error between the actual air flow and the air flow setpoint.

The focus of this paper is on achieving efficient steady state operation and smooth transient response for a highly coupled SOFC and gas turbine system while guaranteeing stability. A PID or other well established linear control schemes, such as LQR, can be used in combination to the reference governor proposed in this paper to increase the response speed. The linear schemes though cannot guarantee stability since as shown in this paper the nonlinearities are dominant. The contribution of the paper, besides the development of a control oriented system model and model-based dynamic analysis, is the design and implementation of a load governor scheme to safeguard the system during transient operation. The proposed algorithm avoids on-line optimization, which often incurs significant computational cost. Avoiding on-line optimization is achieved by leveraging the knowledge of the system dynamics.

## II. SYSTEM OPERATION PRINCIPLE

The hybrid SOFC/GT system analyzed in this work is intended as an auxiliary power unit (APU) for military and commercial applications. It is rated at 30 kW and the key

V. Tsourapas is with Eaton Corporation, Innovation Center, Southfield, MI, [VasiliosTsourapas@Eaton.com](mailto:VasiliosTsourapas@Eaton.com).

J. Sun is with the Department of Naval Architecture & Marine Engineering, University of Michigan, [jingsun@umich.edu](mailto:jingsun@umich.edu).

A. Stefanopoulou is with the Department of Mechanical Engineering, University of Michigan, [annastef@umich.edu](mailto:annastef@umich.edu).

This work is supported in part by the ONR under contract N00014-06-1-0209 and NSF ECS-0501084.

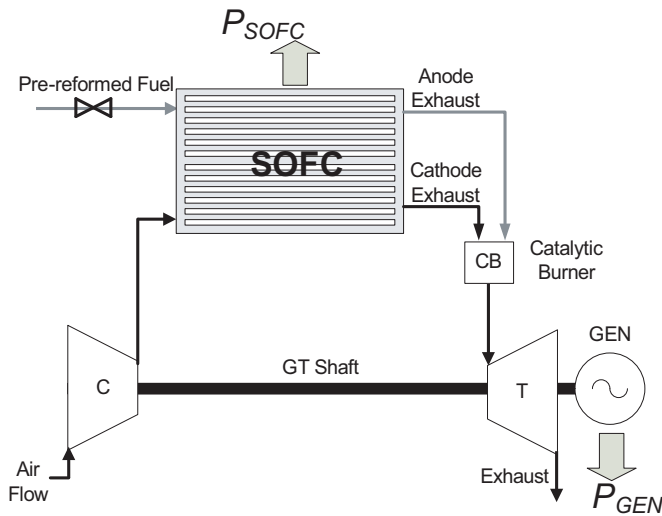


Fig. 1. Hybrid SOFC/GT configuration.

components include a compressor (C), an SOFC stack, a catalytic burner (CB), and a turbine (T) which drives a generator (GEN) as shown in Fig. 1. Other components, such as the reformer and the heat exchangers, are not included in this work in order to focus on the coupling dynamics between the SOFC and the GT. While we believe that the omission of other balance-of-plant components, such as the heat exchangers, does not change the nature of the coupling dynamics between the SOFC and GT, the quantitative effects of temperature coupling introduced by the heat exchangers will be the subject of our future work. The addition of a fuel reformer, on the other hand, will affect the fuel dynamics. In this work, however, we assume that fast fuel delivery is achieved via an accumulator or a tank for pre-reformed fuel, therefore the omission of the fuel reformer does not change the nature of this study.

The air to the SOFC is supplied to the cathode side by a compressor, while fuel is fed to the anode side. The exhaust from the SOFC outlet passes through the CB where the unused fuel is burned to increase the temperature and pressure of the flow. The high temperature and high pressure flow from the CB then powers the turbine, thereby providing a mechanism to recuperate the exhaust energy. The turbine drives both the compressor and the generator through a mechanical shaft; the former delivers the air needed for the SOFC stack operation and the latter provides additional electrical power for the system. The net power output is the sum of the electric power from the SOFC and the generator. In order to explore the dynamic characteristics of the integrated SOFC/GT system, our effort is initially devoted in developing a dynamic model that captures both the steady state and dynamic behavior of the system. The modeling details for components can be found in [1] for the SOFC and in [2], [8] for the CB, GT and the integrated system.

The integrated model has 55 states, of which 52 are the necessary states for capturing the SOFC dynamics from [1],

2 are from the CB and 1 is from the GT shaft dynamics. The input variables to the system are the fuel flow,  $W_f$ , the current drawn from the SOFC stack,  $I_{st}$ , and the generator load,  $P_{gen}^d$ . The optimal setpoints for these inputs to achieve the best system efficiency are determined by an optimization, as elaborated in the next section.

### III. THE SHUTDOWN OF THE OPEN LOOP SYSTEM

In this section, dynamic analysis is performed to understand the open-loop system dynamic characteristics. It is shown that the system is susceptible to power shutdown when an abrupt load increase is applied. The analysis here reveals that the shutdown is initiated by the gas turbine through the shaft dynamic coupling with the SOFC air supply system.

Without any feedback control in place, we consider the open loop response when a demanded load power step, from  $P_{net}=20$  kW to  $P_{net}=21$  kW, is applied. The optimal input settings, identified from the optimization presented in [8], are used to change the fuel flow, the current density drawn from the SOFC and the generator power from 5.8 to 6.2 g/s, 7296 to 7622 A/m<sup>2</sup> and 3.30 to 3.49 kW respectively, synchronized with the change in power demand. It is observed that the system shuts down (namely, the shaft speed  $N$  goes to zero) in about 20 seconds after the steps are applied. For a smaller step though, from 20 to 20.5 kW, the shaft is able to support the applied load and the system reaches the desired net power after 31 seconds. The two trajectories corresponding to the two step responses are shown in Fig. 2.

During the 20 to 21 kW step, the large and sudden increase (step) in the generator load deprives the compressor from having enough power to supply the air during the transient to support the SOFC operation. The sudden increase of load on the shaft first initiates a speed reduction of the shaft, which then causes a decrease in air flow to the SOFC unit that results in reduced exhaust energy out of SOFC. The decrease in the exhaust energy will cause further reduction of the shaft speed, and this positive feedback will lead the turbine shaft to stall and eventually the system to shut down. Therefore, open loop feedforward operation using the optimal steady state setpoints without load rate limiting or load filtering is not an option for rapid load following.

#### A. Transient Response with a Rate Limiter

Given that a rapid increase in the generator load was shown to be the main cause of system shutdown, an intuitive solution is to add a rate limiter to slow down the application of  $P_{gen}^d$ . Multiple rate limits are examined, varying from 3.3 to 6.7 W/s. From Fig. 3, one can see that while the system shutdown is avoided, however, the net power response will depend on the rate limit.

Note that with the open loop feedforward control, the fastest rate limiter on  $P_{gen}^d$  that will not cause shutdown for a 20 to 21 kW step is 6.67 W/s. This rate limit results in a  $P_{net}$  settling time<sup>1</sup> of 168s.

<sup>1</sup>Settling time (ST) in this work is defined as the time required to reach within 10% of the demanded steady state value.

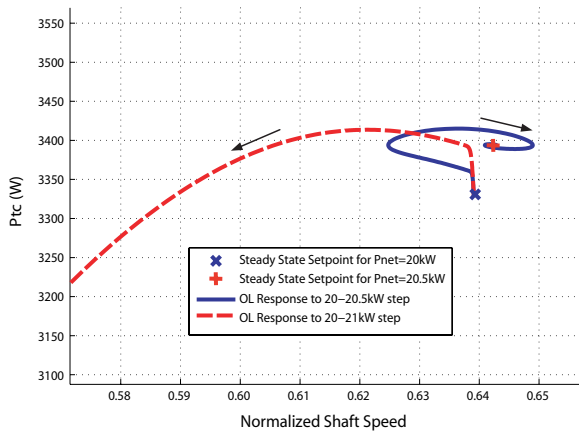


Fig. 2. System response for a 20-20.5 kW and a 20-21 kW step change in net power.

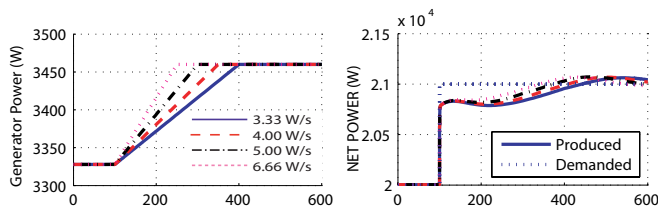


Fig. 3. Step responses from 20 to 21 kW with various rate limiters on  $P_{gen}^d$ .

#### IV. INCREMENTAL STEP REFERENCE GOVERNOR

Guided by the analysis of the shutdown dynamics, we propose a load governor for the generator to throttle the load application whenever necessary to avoid shut down. While the controller is designed based on the reference governor approach found in [9], the novel aspect of this development lies in the implementation algorithm.

##### A. Conventional Reference Governor for the Hybrid SOFC/GT System

For a dynamic system represented by

$$\dot{x} = f(x, u) \quad (1)$$

subject to constraints

$$(x, u) \in O_f \quad (2)$$

the conventional reference governor is an add-on mechanism used to avoid violation of the constraints [10]. Let  $u^d$  be the desired input to the system, the reference governor calculates the optimal feasible input  $u = u^{rg}$  according to:

$$u^{rg}(t + \delta t) = u^{rg}(t) + K(u^d(t) - u^{rg}(t)) \quad (3)$$

where  $K \in [0, 1]$  is determined on-line by solving the following optimization problem:

$$\min_K |u^{rg} - u^d|, \text{ subject to } (x, u^{rg}) \in O_f. \quad (4)$$

This formulation implies that all the constraints are satisfied

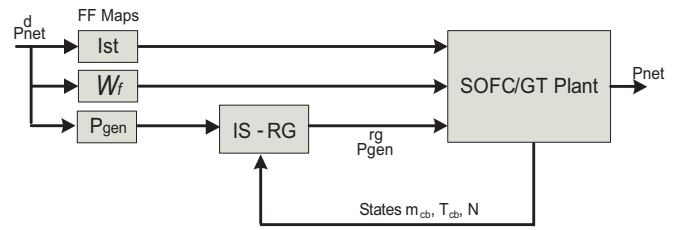


Fig. 4. Schematic of the closed loop SOFC/GT plant with the IS-RG controller.

while the desired reference input is tracked as close as possible.

For the hybrid SOFC-GT system with the feedforward control considered in this study, the external input is the net power demand  $P_{net}$  and a reference governor is incorporated for the generator command  $P_{gen}^d$ , resulting in the closed-loop system shown in Fig. 4. Note that when the net power demand  $P_{net}$  steps up, both the fueling rate  $W_f$  and current drawn from the SOFC  $I_{st}$  will step up according to the feedforward map, while the command to the generator load will be determined by the reference governor to assure system stability.

In the conventional reference governor implementation, the optimization problem (4) subject to the no-shutdown constraint is solved on-line to determine  $K$ . For general nonlinear systems where analytic solutions for the optimization problem are impossible to obtain, this is performed by repeated simulations and one-dimensional search (note that only one variable,  $K$ , is involved in the optimization). For the SOFC/GT system, the conventional reference governor is implemented by simulating the system model repeatedly for different  $K$  in on-line optimization, using bi-sectional search. A transient scenario with a net power demand step up from 20kW to 21kW is considered. For a 500 second input profile (the step is applied at 100sec), it took 38 hours on a laptop computer (Pentium 3 GHz, 2gb RAM) to simulate the system shown in Fig. 4. This computational demand, mainly due to the repeated simulations required for on-line optimization, renders the controller infeasible for our application.

##### B. Incremental Step Reference Governor

To develop computationally feasible load conditioning strategies for the hybrid SOFC-GT system, we propose a novel algorithm referred to as the incremental step reference governor (IS-RG). The ingredients of the proposed algorithm that contribute to the computational efficiency include that (a) the feasibility of the control command is determined based on whether the state belongs to the region of attraction of the corresponding stable equilibrium, rather than through simulations and optimization; and (b) a fixed incremental step, rather than a range of input values, is evaluated to determine the permissibility of load increase. On-line optimization is not performed.

It is noted that the constraint of no-shutdown for transient operation can be expressed in terms of (2), where

$$O_f = R_A(x_{ss}^u) \quad (5)$$

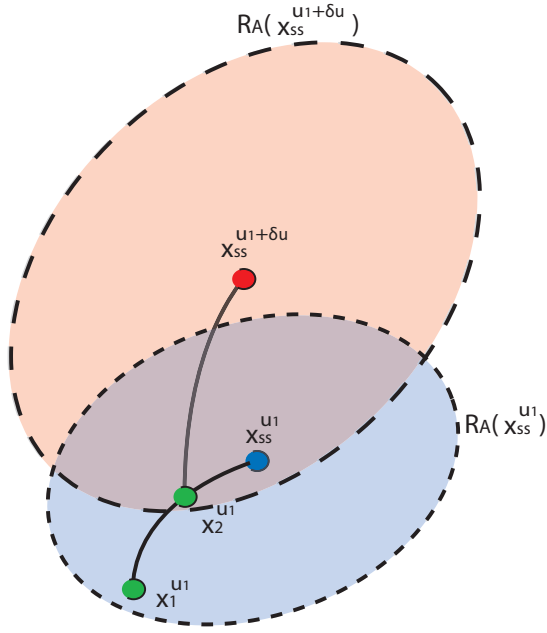


Fig. 5. Schematic explaining the IS-RG principle.

and  $R_A(x_{ss}^u)$  denotes the region of attraction of the stable equilibrium point  $x_{ss}^u$  corresponding to input  $u$ . Here the input  $u$  is the output of the reference governor, namely  $u^d = P_{gen}^d, u = P_{gen}^{rg}$ . The following definition is needed to describe the incremental step reference governor:

**Definition 6.1** *Permissible Incremental Step (IS) Change:*

Given a state  $x_1$  and input  $u$  where  $x_1 \in R_A(x_{ss}^u)$ . If  $x_1 \in R_A(x_{ss}^{u+\delta u})$ , then  $\delta u$  is a permissible IS change.

For the SOFC-GT system, if  $\delta u$  is permissible when  $x(t) = x_1$ , that implies that the generator load can be increased from  $P_{gen}^{rd}$  to  $P_{gen}^{rd} + \delta u$ . Note that for a given  $\delta u$ , whether it is a permissible IS depends on both the state at the time this step will be attempted and the  $u$  (which will determine  $x_{ss}^{u+\delta u}$ ).

A graphic explanation of the permissible incremental step change is shown in Fig. 5. The operating point at time  $t = t_1$  belongs to  $R_A(x_{ss}^{u_1})$  but not to the  $R_A(x_{ss}^{u_1+\delta u})$ , thus  $\delta u$  is not a permissible incremental step at  $t = t_1$ . At time  $t = t_2$  the operating point belongs in  $R_A(x_{ss}^{u_1+\delta u})$ , thus the step change in the input from  $u_1$  to  $u_1 + \delta u$  is permissible.

**Definition 6.2** *Incremental Step - Reference Governor:*

For the dynamic system of the form  $\dot{x}(t) = f(x, u)$ , given the desired input  $u^d(t)$  and  $\delta u = \text{constant}$ , the IS-RG calculates the input  $u(t)$  according to:

$$u(t + \delta t) = \begin{cases} \min [u(t) + \delta u, u^d(t)], & \text{if } \delta u \text{ is a permissible IS;} \\ \min [u(t), u^d(t)], & \text{if } \delta u \text{ is not a permissible IS} \end{cases} \quad (6)$$

where  $u(t + \delta t)$  denotes the input to be applied at the next time step after  $t$ .

The IS-RG applies incremental steps to the reference command until the final desired setpoint  $u^d$  is reached. To

guarantee that the desired setpoint will be reached, i.e.,

$$\lim_{t \rightarrow \infty} u(t) = u^d,$$

a sufficient condition is that  $\delta u$  is chosen such that:

$$x_{ss}^{u_0+k\delta u} \in R_A(x_{ss}^{u_0+(k+1)\delta u}), k = 0, 1, 2, \dots, \quad (7)$$

where  $u_0$  is the initial control input. Namely, the equilibrium corresponding to the current input,  $u_0 + k\delta u$ , should belong to the region of attraction corresponding to the equilibrium with  $u_0 + (k + 1)\delta u$ . Condition (7) can be satisfied by choosing  $\delta u$  to be sufficiently small. If an intermediate equilibrium,  $x_{ss}^{u_i}$  does not belong to the region of attraction of the next equilibrium, we run into the possibility of reaching an intermediate equilibrium where the load cannot be increased any further by the incremental amount specified by  $\delta u$ . It is shown later that a small  $\delta u$  will not slow down the system as long as the sampling time is relatively fast compared to the system dynamics.

The main advantage of the proposed IS-RG is that it converts an optimization problem (i.e., determining  $K$  for (4)) into the problem of checking whether  $\delta u$  is a permissible step at each time, or equivalently, whether the state  $x$  belongs to  $R_A(x_{ss}^{u+\delta u})$ , where  $(x, u)$  is the current state and the generator load respectively. The latter problem can be solved much more easily if one can find a way to characterize the region of attraction as a function of the input.

For the SOFG/GT system described in this paper, however, the region of attraction corresponding to each input value is characterized by 55 states, and the measurement of all states has to be used online to check whether  $\delta u$  is a permissible step if (6) is implemented as it is. This is neither necessary nor desirable, as we know that some states will not be important in deciding the feasible input step size. In the sequel, we propose to characterize the region of attraction used for IS-RG implementation using a physics-based nonlinear reduced order model and show that only 3 state measurements are required to describe the  $R_A$  of the SOFC/GT system while the remaining 52 states can be neglected.

### C. Reduced Order Model and $R_A$ Characterization

In this section, we describe a reduced order model (ROM) that allows us to characterize the region of attraction in a low dimensional space to facilitate the IS-RG implementation. Three states: the mass of the catalytic burner, the temperature of the catalytic burner and the shaft rotational speed have been identified to be the key states by linearizing the plant at various load operating points, then normalizing the inputs, outputs and states and finally by performing a balanced realization. The resulting balanced realization shows these three states as the dominating ones, separating from the rest of the states. The selection of these states can also be justified physically given that they define the energy delivered to the turbine and thus they dictate the shaft dynamics. Note that the reduced order model with 3 states will not capture some characteristics of the full order model, such as the

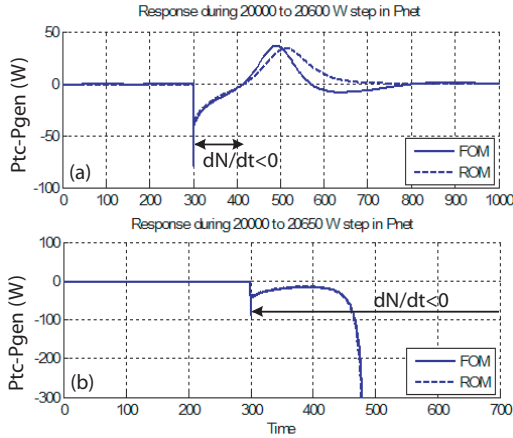


Fig. 6. Comparison of the reduced and full-order model responses to load steps change.

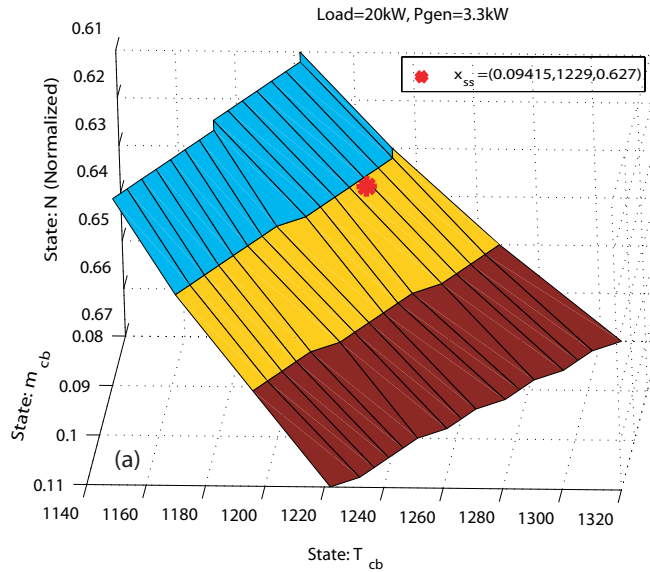


Fig. 7. Boundaries of  $R_A$  for  $P_{net} = 20$  kW.

current distribution, the main goal for this ROM is to capture the shutdown dynamics of the full order model (FOM). A detailed description of the nonlinear ROM composed of the key states can be found in [2].

Comparing the response of the FOM and the ROM in terms of the shaft power, the two model match well as shown in Fig. 6. Most importantly, the shutdown effect is captured during a 660W step as shown in Fig. 6c. Note that during the period of time when the shutdown can occur (i.e., when  $\dot{N} < 0$  or  $P_{tc} - P_{gen} < 0$ ), the behavior of the FOM and ROM is almost identical as shown in Fig. 6.

Based on the ROM and FOM analysis, we characterize the  $R_A$  of the FOM in terms of the dominant states  $m_{cb}$ ,  $T_{cb}$  and  $N$  for the range of loads. The remaining states have negligible effect on the  $R_A$ , i.e., the 55-dimension  $R_A$  can be collapsed into a 3-dimension  $R_A$ . This result is also numerically verified for selected load conditions. The  $R_A$  plot for  $P_{tc} = 20$  kW, together with the corresponding stable

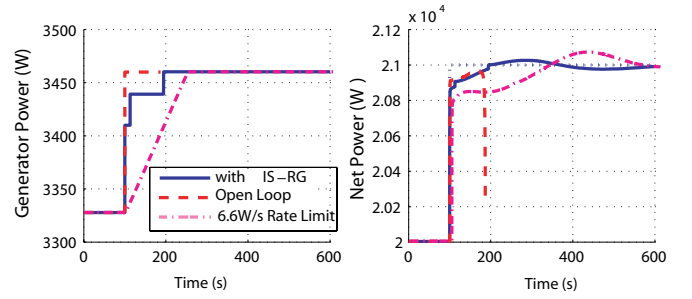


Fig. 8. Open and closed loop (with IS-RG) responses to a load step change from 20 to 21 kW.

equilibrium point, is shown in Fig. 7. The boundary surface shown in Fig 7(a) divide the 3-dimensional space into two regions, a  $(T_{cb}, m_{cb}, N)$  point is considered to be within the region of attraction if it is on the same side as the equilibrium point.

To better assist readers to view the  $R_A$  plot, the 2-dimensional plots are also given in Fig 7(b), with  $N$  fixed as a parameter. For each  $N$ , the curve on Fig 7(b) divides the plane into two regions: the upper-right part is within the region of attraction, while the lower-left part is outside.

The boundaries of the  $R_A$  (i.e., each of the curves shown in Fig.7(b)) can be approximated by a linear function of the form:

$$T_{cb}^{P_{net}} = a^{P_{net}}(N) \cdot m_{cb} + b^{P_{net}}(N). \quad (8)$$

The parameters  $a^{P_{net}}(N)$  and  $b^{P_{net}}(N)$  are calculated for different shaft speeds at each  $P_{net}$  and are stored as lookup tables, indexed by  $N$  and  $P_{net}$ , for online implementation.

#### D. Implementation of the IS-RG for the SOFC/GT System

Utilizing the  $R_A$  calculated offline and stored for online look up, the IS-RG controller safeguards the system with a minimum online computational requirement. Fig. 8 shows the simulation of the closed loop FOM with IS-RG for a 20 to 21 kW step increase in the desired net power, where  $\delta P_{gen}$  is chosen as 20 W. Note that for the same step, the open loop system (without the IS-RG) shuts down shortly after the step is applied (dashed line in Fig. 8), while the open loop system with a  $P_{gen}$  rate limiter exhibits a settling time of 168 sec. The settling time achieved the IS-RG is about 76 sec, which is comparable to 75 sec achieved by the conventional reference governor, but it represents a significant improvement compared to the rate limiter. The required simulation time is 145sec compared to the 38hours for the conventional reference governor for this 500 sec run time. Note that the size of  $\delta P_{net}$  is set to 20 W to ensure that condition (7) is met.

It should also be noted that the main function of the IS-RG is to avoid shutdown. This is achieved by slowing down the application of the generator load to ensure safe operation. It does not attempt to change the dynamics of the system. In order to enhance the performance, the IS-RG controller will be combined with a proportional controller in future work that regulates the fuel flow into the CB during a transient to

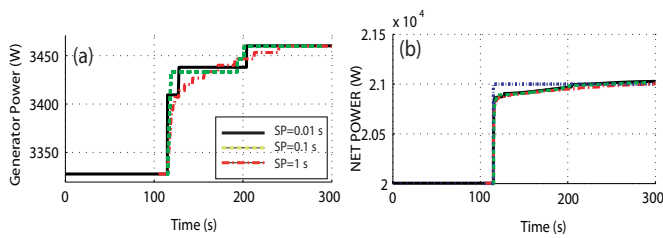


Fig. 9. IS-RG response with various sampling periods (SP)

increase the energy input into the turbine, thereby helping sustain the applied load.

### E. Effects of the Sampling Period (SP)

Since the incremental step is applied whenever it is deemed feasible by the IS-RG at each sampling instant, the sample period of the controller will also affect the controller performance and computational requirements for the IS-RG implementation. While fast sample may help improve the power response, it will also increase the computational load. In this subsection, the effects of the sampling period (SP) of the controller on the system performance will be examined to understand the trade-offs.

In our implementation, the controller is discretized using a sampler in the input (measurements) and a zero-order hold at the output (reference command). The sampling period of the controller, for the simulation results shown in Fig 8, is variable and determined by Matlab/Simulink©. On average, Matlab/Simulink© sets the sampling time of the controller during the transient equal to 0.01 s (i.e., 100 Hz). Figure 9, shows the system response for a 20 to 21 kW step for 0.01 s, 0.1 s and 1 s sampling periods and  $\delta P_{net} = 20$  W.

It can be seen that for sampling frequencies of 100, 10 and 1 Hz, the system's settling time during a 20 to 21 kW step increase in load is 76, 77 and 83 s, respectively (see also Table I for the summary. This simulation shows that for a 10 times increase in the IS-RF sampling period, the settling time deteriorates by 1%, while for a 100 times increase in sampling period, the settling time deteriorates by 9%. This result confirms that, without requiring high sampling frequency, the IS-RG can achieve the performance at the desired level. Furthermore, reducing the sampling frequency will reduce the computational load. This computational load reduction, however, is not very noticeable in our simulation when the plant and controller are simulated on the same CPU, as summarized in Table 1.

## V. SUMMARY AND CONCLUSIONS

In this paper, the efficiency and the transient operation of a hybrid Solid Oxide Fuel Cell (SOFC) and Gas Turbine (GT) system are analyzed. A nonlinear, control oriented model is developed and used initially for defining, via optimization, the fuel, current and generator load setpoints that yield the highest system efficiency. However, utilizing these setpoints for load transitions is shown to cause system shutdown when large and fast transitions are attempted. The shutdown

Control Type	Settling (s)	Simulation Time (min)
Open Loop	-	2.1
Rate Limiter	168	2.4
IS-RG (1 Hz)	83	2.2
IS-RG (10 Hz)	77	2.2
IS-RG (100 Hz)	76	2.3
Conventional RG (100Hz)	75	1800

TABLE I

COMPARISON OF SETTLING TIMES AND SIMULATION TIMES FOR DIFFERENT OPEN AND CLOSED LOOP SCHEMES RESPONDING TO A LOAD STEP FROM 20 TO 21 kW.

phenomenon is analyzed and the fast coupling dynamics between the fuel cell and the gas turbine are identified as the main cause for the shutdown phenomenon.

To mitigate the shutdown problems associated with the open loop operation, an IS-RG control scheme is developed and implemented to modify the application of the generator load. Slowing down the application of the generator load allows more power delivered to the shaft during transients, thereby preventing a large rotational speed drop of the shaft. The IS-RG achieves the constraint enforcement without compromising tracking performance and without using online optimization.

## REFERENCES

- [1] H. Xi, "Dynamic modeling and control of planar sofc power systems," *University of Michigan, Department of Naval Architecture and Marine Engineering, Ph.D. Thesis*, 2007.
- [2] V. Tsourapas, "Control analysis of integrated fuel cell systems with energy recuperation devices," *University of Michigan, Department of Naval Architecture and Marine Engineering, Ph.D. Thesis*, 2007.
- [3] P. Kuchonthara, S. Bhattacharya, and A. Tsutsumi, "Energy recuperation in solid oxide fuel cell (sofc) and gas turbine (gt) combined system," *Journal of Power Sources*, vol. 117, p. 713, 2003.
- [4] X. Wang, B. Huang, and T. Chen, "Data-driven predictive control for solid oxide fuel cells," *Journal of Process Control*, vol. 17, pp. 103–114, 2007.
- [5] R. A. Roberts and J. Brouwer, "Dynamic simulation of a pressurized 220 kw solid oxide fuel-cell gas-turbine hybrid system: Modeled performance compared to measured results," *Journal of power sources*, vol. 3, pp. 18–25, 2006.
- [6] C. Wchter, R. Lunderstdt, and F. Joos, "Dynamic model of a pressurized sofc/gas turbine hybrid power plant for the development of control concepts," *Journal of Fuel Cell Science and Technology*, vol. 3, pp. 271–279, 2006.
- [7] C. Stiller, B. Thorud, O. Bolland, R. Kandepu, and L. Imsland, "Control strategy for a solid oxide fuel cell and gas turbine hybrid system," *Journal of Power Sources*, vol. 158, pp. 303–315, 2006.
- [8] V. Tsourapas, J. Sun, and A. Nickens, "Control oriented modeling and analysis of a hybrid solid oxide fuel cell and gas turbine (sofc/gt) system," *ASME Conference on Fuel Cell Science and Technology*, no. FC-07-1086, 2007.
- [9] J. Sun and I. Kolmanovsky, "A robust load governor for fuel cell oxygen starvation protection," *IEEE Transactions of Control Systems*, vol. 13, pp. 911–920, 2005.
- [10] I. V. K. E. Gilbert and K. T. Tan, "Discrete time reference governors and the nonlinear control of systems with state and control constraints," *International Journal of Robust and Nonlinear Control*, vol. 5, pp. 6487–504, 1995.